ELSEVIER

S0032-3861(96)00320-5

Polymer Vol. 37 No. 21, pp. 4695–4704, 1996

0032-3861/96/$15.00 + 0.00

Imaging of epitaxially grown poly(*p*-oxybenzoate) films with the atomic force microscope

Jing Wang, Akira Kaito*, Satomi Ohnishi, Kiyoshi Yase and Nobutaka Tanigaki

National Institute of Materials and Chemical Research, 1–1 Higashi, Tsukuba, Ibaraki 305, Japan

(Received 18 September 1995; revised 31 January 1996)

Characterization of poly(*p*-oxybenzoate) (POBA) films epitaxially grown on mica and KBr single crystal substrates was performed by atomic force microscopy (AFM). For a thin POBA film sample prepared at 320°C on a mica substrate, oligomer domains were found in the vicinity of the nuclei, forming an interfacial layer between the mica crystal and the homogeneous POBA film. The AFM study further clarified the lateral crystal growth mechanism of POBA. On POBA films with a thickness ranging from 100 to 200 nm on mica KBr substrates, small lateral singular domains with dimensions of 50–100 nm composed the large orientation domains. The size of the singular domains increased with the POBA film thickness. On POBA films beyond 300 nm in thickness on mica and KBr substrates, orientation domains were singular domains, some of which were bounded by vicinal planes. Copyright © 1996 Elsevier Science Ltd.

(Keywords: atomic force microscopy; poly(p-oxybenzoate); epitaxial crystal growth)

INTRODUCTION

Atomic force microscopy (AFM), developed since 1986, is capable of imaging film surface with atomic resolution as well as scanning tunnelling microscopy (STM), and has the advantage that AFM may be applied to nonconducting substrates and is not limited by the film thickness of the sample[1,2].

Poly(*p*-oxybenzoate) (POBA) is one of the stiff-chain polymers which are able to form needle-like whisker crystals during *in situ* polymerization. It is generally accepted that the POBA crystal whiskers are grown from short chain oligomers which crystallize out of solution with a degree of polymerization (DP) of 6–8[3]. Further chain growth occurs by simultaneous crystallization and polymerization of oligomers onto the chain ends exposed on the surface of the crystal structure. In this work, POBA films on single crystalline substrates were prepared under essentially the same conditions for which POBA crystal whiskers form.

The POBA chain conformation consists of two types: *cis* and *trans*[4] (see *Figure 1*). Both experimentally and theoretically, it is found that the rod-like *trans* form is stable for oligomers and the crankshaft-like *cis* form is stable for the long polymer chains[5]. Recently, proposed models of molecular packing in the three crystal phases of POBA based on total energy calculations suggest that the chain confirmation is *trans* for phase II and *cis* for phases I and III[4].

In our previous study, we achieved epitaxial growth of POBA on mica and KBr single crystal substrates by *in situ* polymerization. The *c*-axis of POBA crystals aligns parallel to the substrate surface with azimuthal orientations[6]. On very thin films of POBA on mica, POBA nuclei growing on mica have been observed. This paper reports the characterization of the epitaxially grown POBA films by AFM. By applying AFM to scan the low area near the nuclei, POBA oligomer domains were discovered adsorbed on the mica surface. An AFM study on the films with thickness far beyond monolayer growth revealed a lateral crystal growth mechanism.

A molecular model to describe the epitaxial relationship between the POBA oligomers and the mica crystal lattice is proposed by referring to the molecular packing in crystal phase II of POBA with consideration of the interaction between POBA and mica.

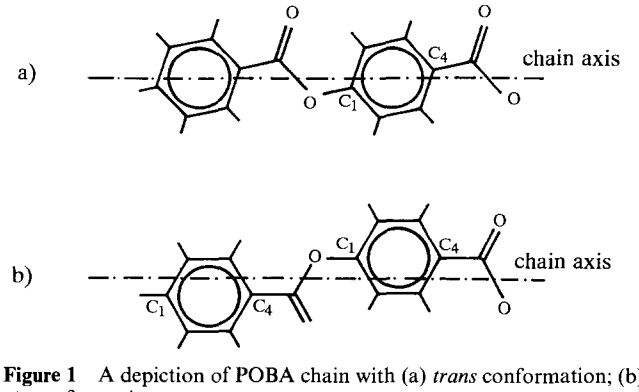

Figure 1 A depiction of POBA chain with (a) *trans* conformation; (b) *cis* conformation

* To whom correspondence should be addressed

Table 1 Reaction conditions and film thickness

Sample no.	Substrate	Reaction condition	Film thickness (nm)
1	mica	320°C, 7 h	thin[a]
2	mica	320°C, 7 h	80–100
3	mica	320°C, 7 h	300–400[b]
4	KBr	320°C, 7 h	110–150
5	KBr	320°C, 7 h	470–640

[a] The film is so thin that the thickness cannot be determined
[b] The film thickness of Sample 3 was measured mechanically, while the rest of the samples were related to Sample 3 by the absorption peak ratio of *FT*i.r. spectra

EXPERIMENTAL

4-Acetoxybenzoic acid was polymerized in paraffin solution under an argon flow. The monomer was purified by recrystallization from butyl acetate. Mica and KBr were freshly cleaved under a nitrogen atmosphere and were put into the reaction flask. After the reaction, the substrates were washed with diethylether and finally dried in a vacuum oven at 100°C for 4 h. The reaction conditions of the samples are summarized in *Table 1*.

Transmission electron microscopy (TEM) was observed with a Zeiss CEU-902 equipped with a Casting-Henry electron energy filter. The accelerating voltage was 80 kV.

The AFM system used in this study was a NanoScope II (Digital Instruments, Inc.). The D-scanner with a scan range about $12 \times 12\,\mu m$ was used. The $200\,\mu m$ long cantilevers with a nominal spring constant of $0.12\,Nm^{-1}$ and Si_3N_4 tips were purchased from Digital Instruments. AFM images (400×400 pixels) were obtained using 'height mode', which kept the force constant, in air at room temperature. Typical parameters for the measurements were as follows: integral gain = 3; proportional gain = 5; two-dimensional gain = 0.3; scan rate = 19.6 Hz; scan width = 5000–8000 nm. In order to obtain the best imaging, the applied force was adjusted to the desired strength for the experiment, typically around 10–50 pN in the repulsive range.

RESULTS AND DISCUSSION

AFM. observations were performed on three samples of POBA on mica substrates and two samples on KBr substrates.

POBA films on mica substrate

Mica has a layered structure. The crystal lattice structure of mica is shown in *Figure 2*. The mica surface after cleaving consists of a sheet of oxygen atoms in pseudo-hexagonal symmetry which is bonded by an underlying layer of silicon atoms[7]. The crystal lattice of mica is monoclinic with a rectangular *ab* plane parallel to the surface, having [100], [110], and [1$\bar{1}$0] axes parallel to the three edges of the pseudo-hexagonal symmetry. A freshly cleaved mica surface is lightly negatively charged[8].

Sample 1 (mica) is the same as Sample 1 in the previous paper[6]. Because the film of Sample 1 was very thin, uncovered mica surfaces were ubiquitous microscopically although an uniform thin layer of the POBA film was perceived macroscopically. *Figure 3* shows the AFM photograph of Sample 1. The POBA nuclei are observed in the AFM photograph. The thin layers of POBA crystals were observed in the vicinities of nuclei, whereas the uncovered surface of mica was found in the area distant from the nuclei. AFM experiments on Sample 1 were performed mainly in two locations (*Figures 4* and *5*). In each location, the AFM images were taken within the range of 2–3 μm, and the sample was moved only in the X and Y directions without rotation during the AFM measurements. The polarized optical microscopy shows that the size of single crystal domain having the common optic axis is of the order of 10 mm. The AFM image was taken after removing the surface layer of samples by the tip, and the experiment confirmed that the crystal axis of mica does not vary with the positions in the X and Y directions. Thus an AFM photograph of mica on the uncovered area was taken in each location to offer a reference for the directional matching of the molecular arrangement between the substrate and the POBA film.

The AFM image of uncovered mica surface is shown in *Figures 4a* and *5a*. As the AFM images of mica display only hexagonal symmetry of oxygen arrays, one edge of the hexagon could be parallel to any of the [100] and [110] or [1$\bar{1}$0] axes of mica. We refer arbitrarily to one

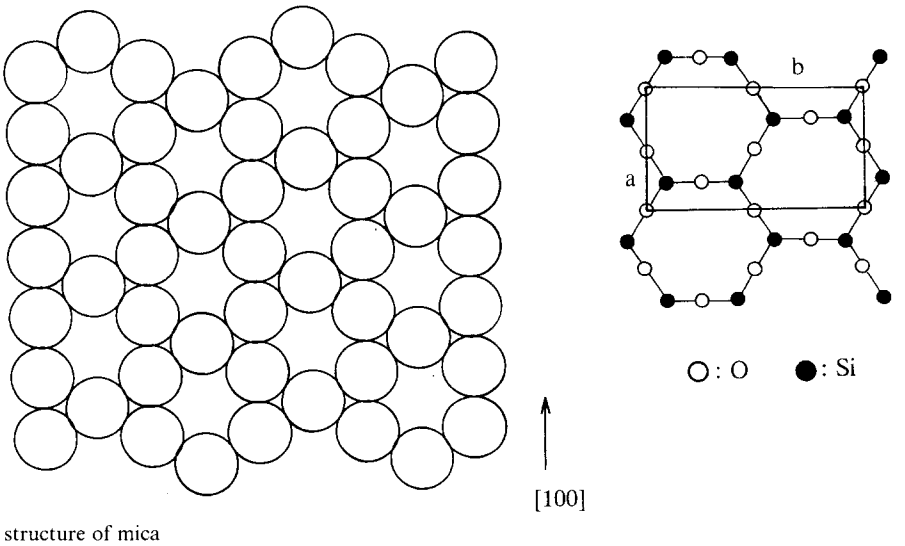

Figure 2 Crystal lattice structure of mica

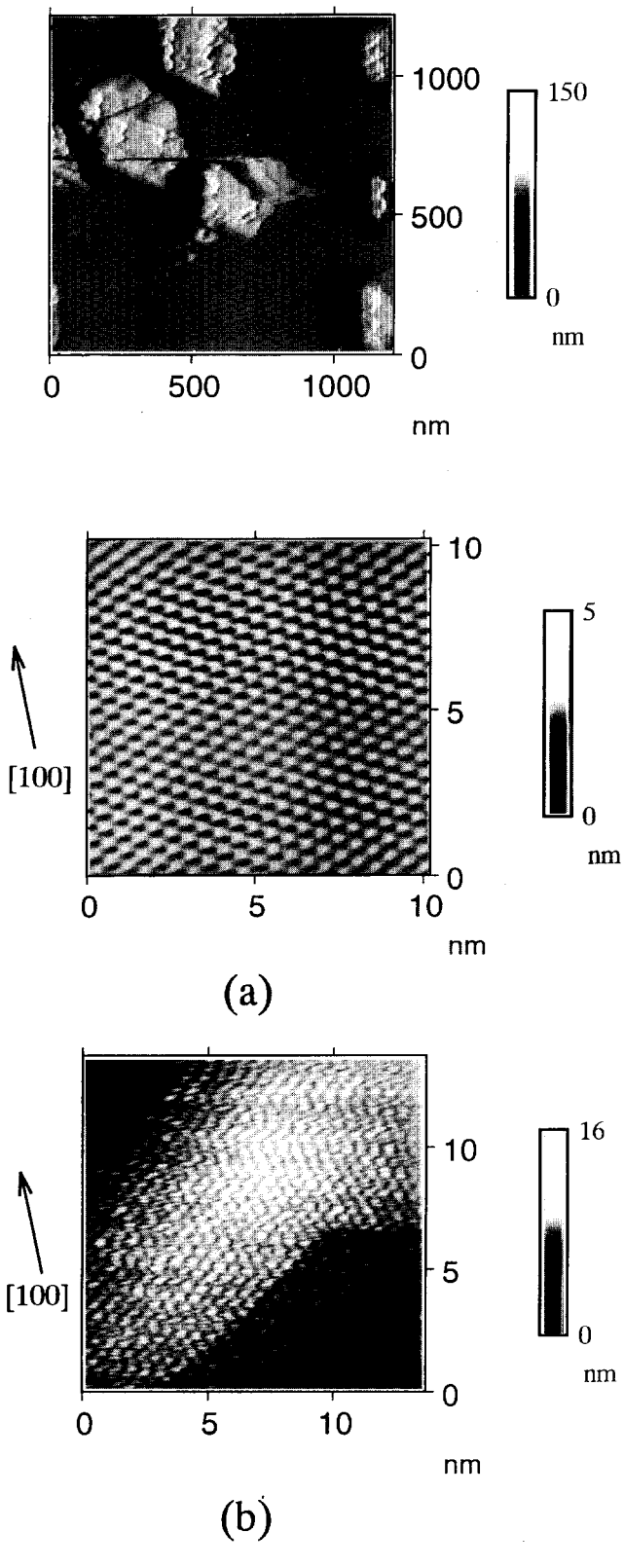

Figure 4 (a) AFM image of uncovered mica surface in Sample 1; (b) AFM image of thin POBA layer in Sample 1 (mica) taken in the vicinity of nuclei (see *Figure 3*)

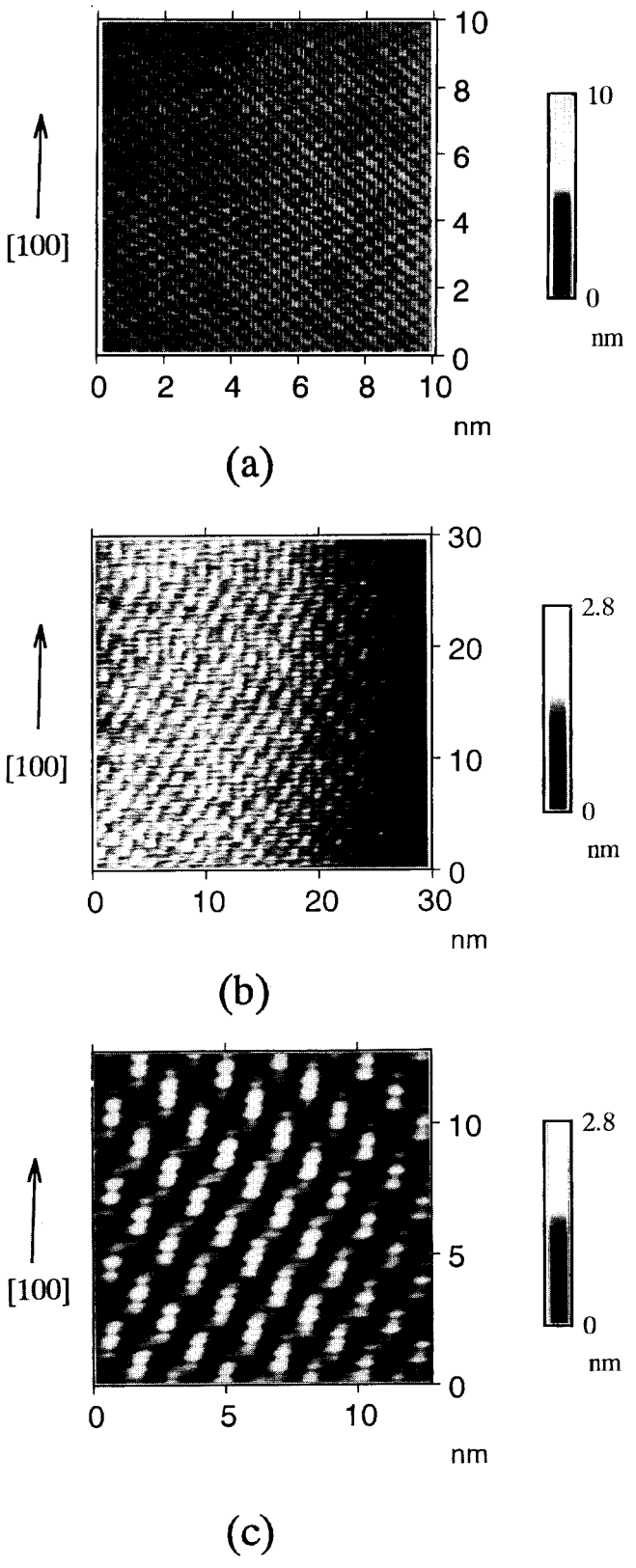

Figure 5 (a) AFM image of uncovered mica surface on Sample 1; (b) AFM image of thin POBA layer in Sample 1 (mica) taken in the vicinity of nuclei; (c) Fourier-filtered image of *Figure 5b*

edge as the [100] axis of mica in *Figures 4a* and *5a* for convenience.

An AFM image in *Figure 4b*, which was scanned in the vicinities of the nuclei in *Figure 3*, frequently shows the POBA growth in a zig-zag pattern which is in contrast to the usual POBA chain packing on a mostly phase I crystal lattice observed explicitly by AFM in the thicker samples. During this imaging, the forces acting on the tip of $10^{-8} - 4 \times 10^{-8}$ N were calculated from the force curves. The straight chain length of the zig-zag patterns

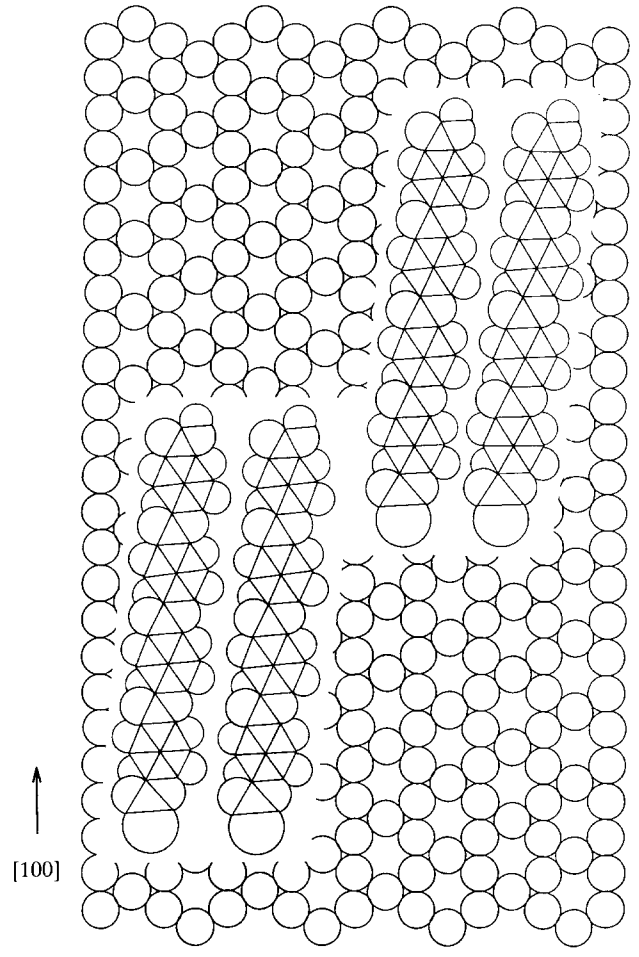

Figure 6 A molecular model of POBA oligomers on hexagonal oxygen arrays of mica

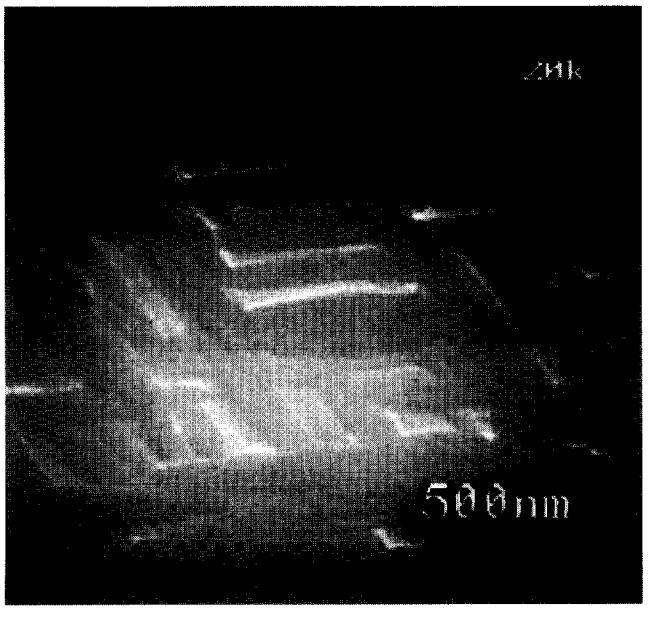

Figure 7 TEM photograph of Sample 2 (mica)

is 1–8 nm, which corresponds to 2–16 repeating units of POBA. The zig-zag path, which is considered to be parallel to the chain axis of the POBA oligomers, is always parallel to one of the edges of the hexagonal

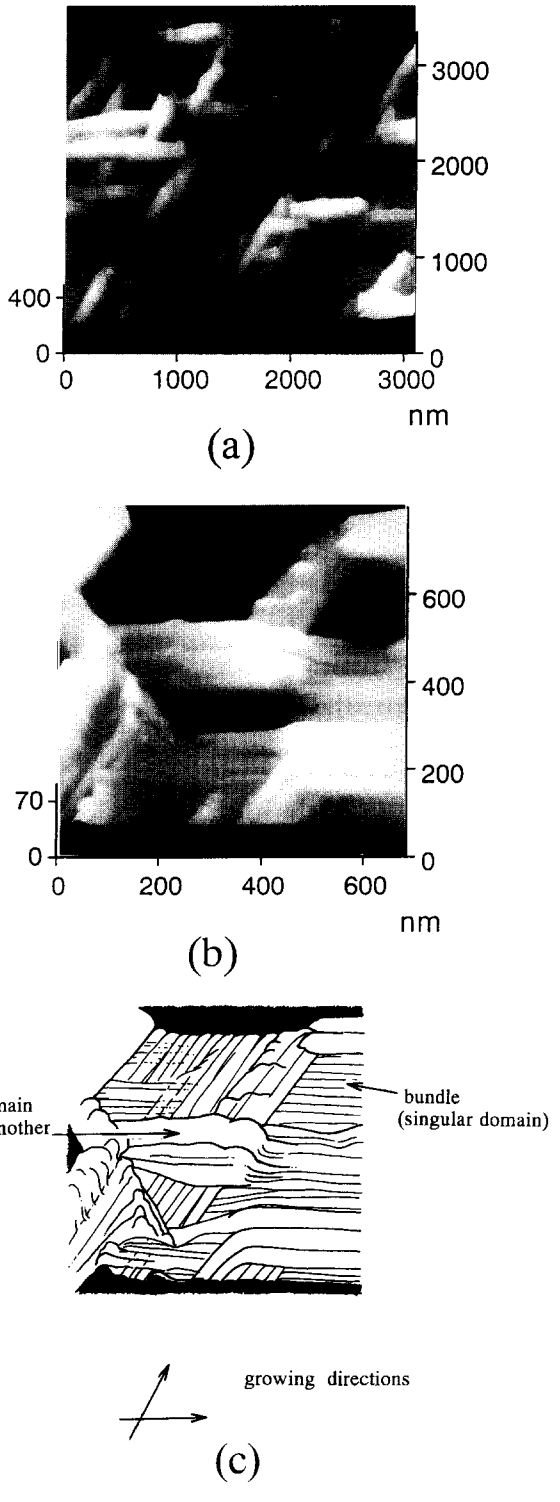

Figure 8 (a) AFM image of Sample 2 (mica); (b) AFM image of Sample 2 (higher magnification); (c) schematic drawing of crystal morphology of Sample 2 (mica)

symmetry of mica. The interchain spacing is in the range of 0.45–0.5 nm, which corresponds to the crystal lattice spacing d_{110} of POBA crystal. It may be seen in *Figure 4b* that the step of cleaved mica is marked by clear straight lines. Yet uninfluenced by the step, POBA oligomers align in two directions, which are parallel to the two edges of hexagonal symmetry of mica, in the lower part of the AFM image. Also, from the estimation of the transverse width of each POBA oligomer block,

POBA oligomers in *Figure 4b* space individually and uniformly.

The AFM photograph of POBA in *Figure 5b* was scanned at another location vicinal to one of the nuclei. *Figure 5b* shows basically long cylinder-like domains with dimensions of about 1.07 nm in width and 2.62 nm in length. Combining the information from *Figure 5(a* and *b)*, the long axis of each domain in *Figure 5b* inclines slightly to the right of the [100] axis of mica. Furthermore, the domains line up at a 30° angle from the [100] axis of mica.

The same picture in *Figure 5b* after Fourier filtering in shown in *Figure 5c*. *Figure 5c* clearly shows that each domain actually consists of four units ascending up slightly to the right in a staircase pattern. The vertical length of each unit is roughly the distance of one repeat unit of the POBA polymer chain. As the inclination of the long axis in *Figure 5c* has been adjusted by steps, the vertical axis of each unit is precisely parallel to the [100] axis of mica. In addition, the first unit in each domain overlaps horizontally with the last unit of the vicinal domain. The sum of the width of the two units is about 1.62 nm. As we see, the width of each unit in the middle sections of the long cylinder is about 1.05 nm. The width of the oligomer units in *Figure 5c* is roughly twice as wide as that of the oligomers in *Figure 4b*.

In contrast to the usual POBA chain packing on a mostly phase I crystal lattice observed explicitly by AFM in the following samples, both the domain phenomenon and the pattern of the domains reported here are believed to be the unique result of their growth on a single crystal lattice of mica. We consider that these are monolayer oligomer domains. Each domain contains two oligomers with repeat units of four in the *trans* conformation. As shown in *Figure 1*, the repeat unit of POBA chain is about 0.62 nm, which is half length of the *c*-axis. The lengths of the oligomers are shorter than the generally expected six to eight repeat units before oligomers precipitate out at the reaction temperature of 320°C[3]. These short chain oligomers probably precipitated out at the beginning of the reaction at temperatures lower than the final 320°C. As the temperature approached or reached 320°C, the oligomers were adsorbed onto the mica surface before being redissolved back to the solution.

A possible molecular model of POBA oligomer arrangement in relation to the mica hexagonal oxygen symmetry is proposed (*Figure 6*). The features of the model are summarized as follows:

1. Because the *trans* form is a more stable conformation

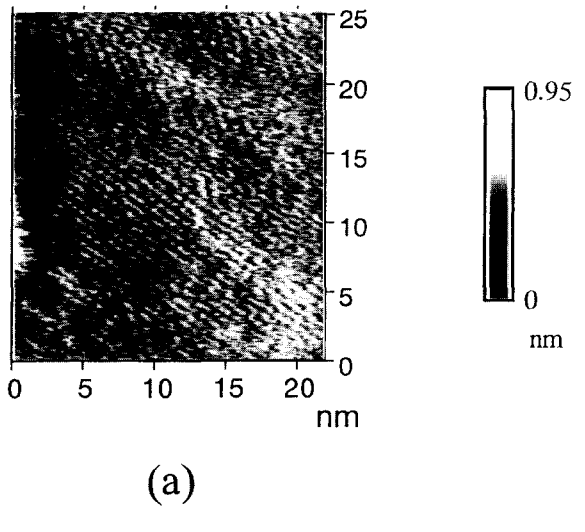

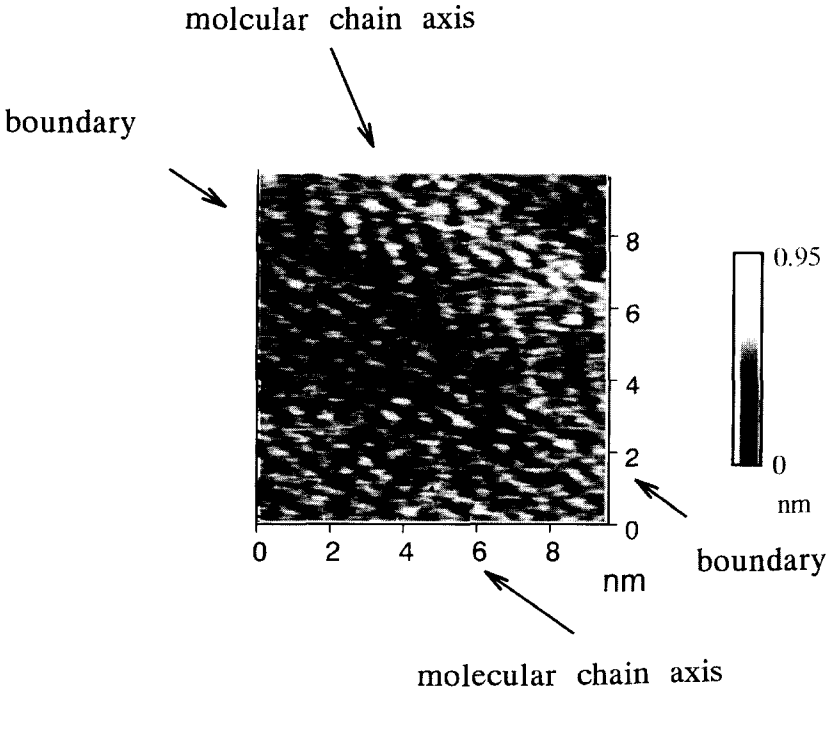

Figure 9 High resolution AFM image of Sample 2 (mica)

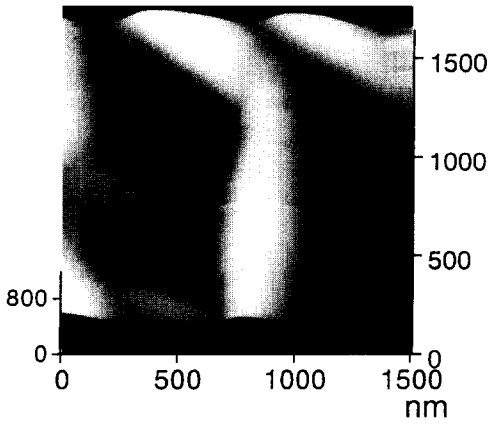

Figure 10 AFM image of Sample 3 (mica)

for the oligomers than the *cis* form[5], the oligomers have a *trans* conformation that fits the staircase pattern in the domain.

2. The C_1–C_4 axis of each phenylene ring in the oligomer is parallel to the [100] axis of mica. This apparent match with the AFM image is also consistent with the fact that long-chain POBA in the phase I arrangement has a *c*-axis parallel to the [100] and [110] axes of mica as in the case of Samples 2 and 3.
3. Because each oligomer has one carboxylic acid group on one end, which is capable of forming hydrogen bonds with vicinal oxygen on the carbonyl group, there might be intermolecular hydrogen bonds between two oligomers in the same domain as well as between the last unit of one oligomer domain and the first unit of the next domain (*Figure 6*). The hydrogen bonds might contribute to the close association between the two vicinal domains.

Consequently, at least in certain regions, oligomer domains form the interfacial plane between the mica surface and the three dimensional nuclei growth of POBA. As we recall, thermodynamic considerations permit three different modes of epitaxial nucleation according to the value of adhesion energy[9]. The first two growth modes are two-dimensional (2D) modes which differ from each other only after the first monolayer 2D growth in either continuing layer by layer growth (Frank Van der Merwe mode) or followed by a three-dimensional (3D) growth (Stranski–Krastanor mode). The third growth mode (Volmer Weber mode) has 3D epitaxial nuclei form directly on the substrate. A high

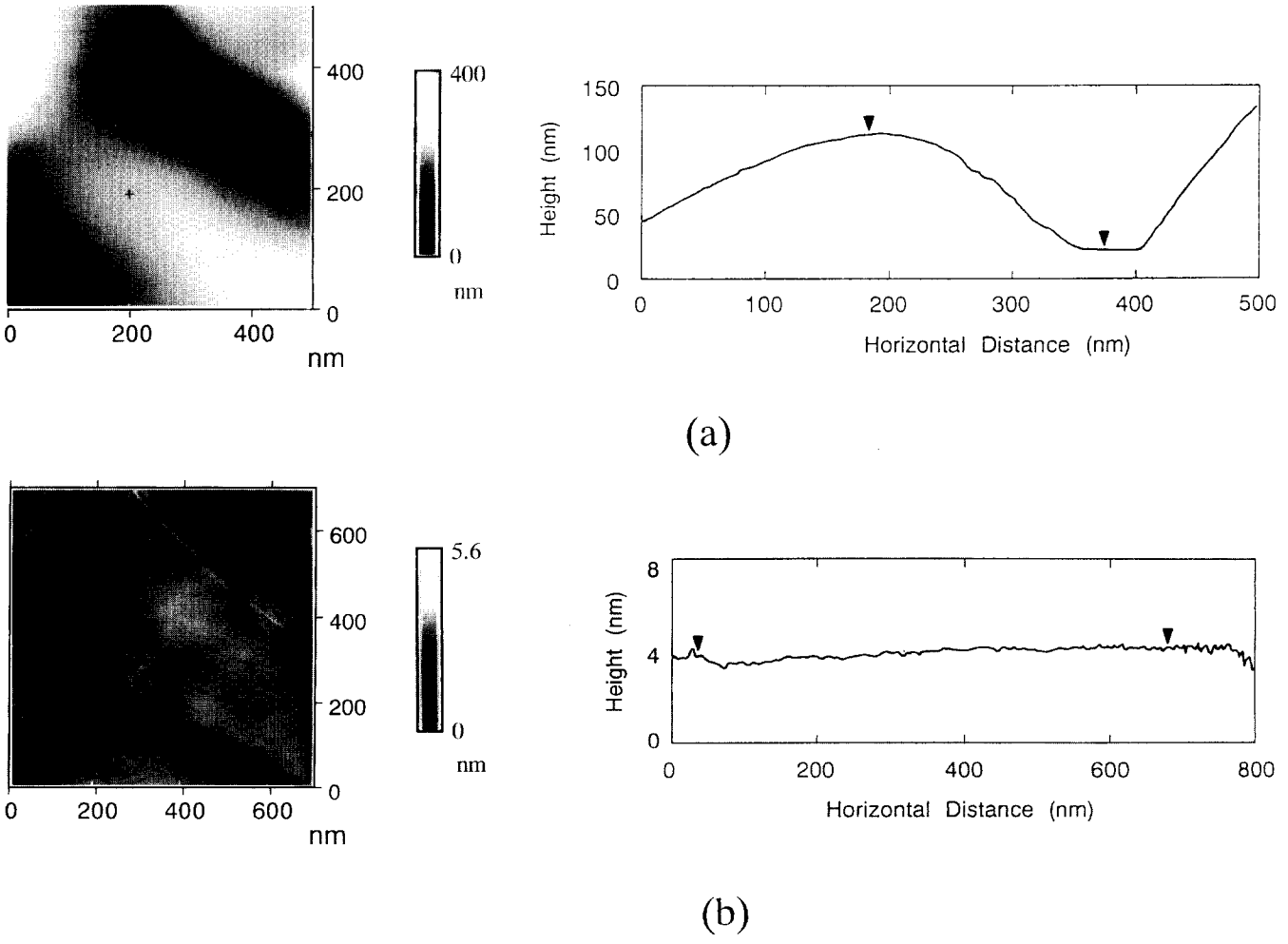

Figure 11 AFM images and surface profiles of Sample 3 (mica). The cross-sectional views between two crosses are shown in the above, where right and left arrows correspond to the crosses

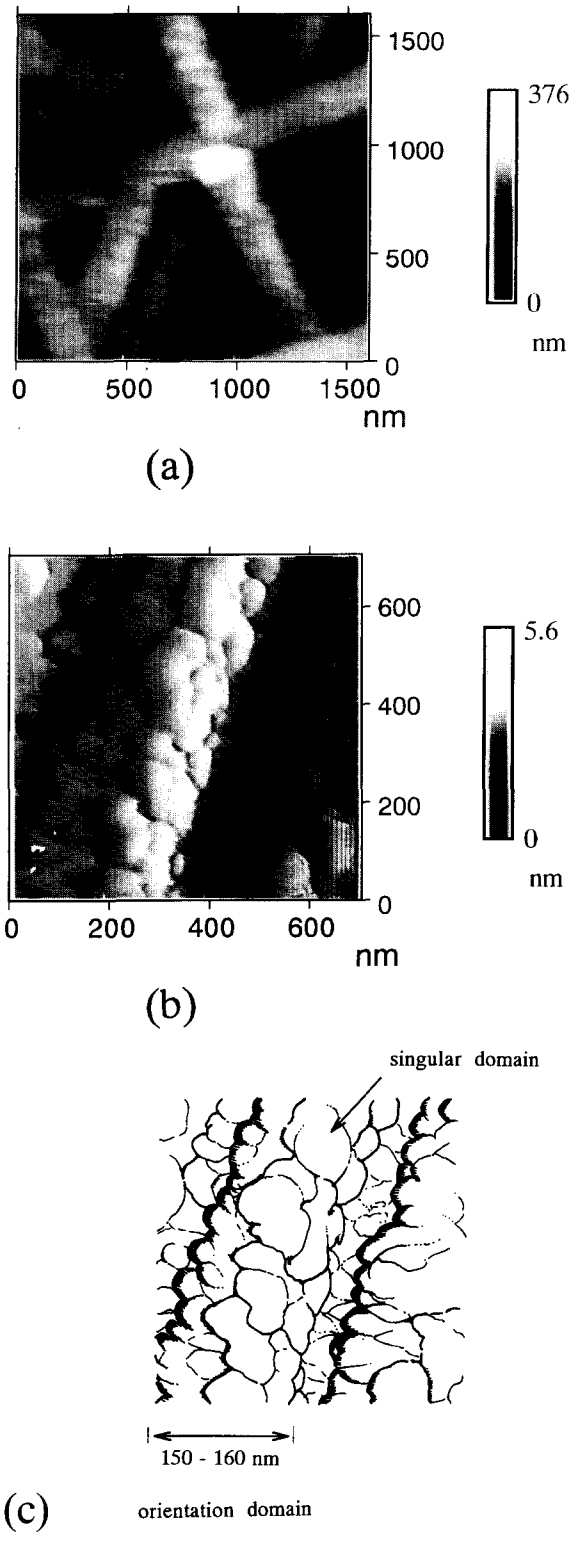

Figure 12 (a, b) AFM images of Sample 4 (KBr); (c) schematic drawing of the crystal domain structure of Sample 4 (KBr)

adhesion energy between the two phases is critical for 2D epitaxial growth. Apparently the Stranski–Krastanor mode describes the POBA epitaxial growth on mica well, in which oligomer domains form the first monolayer followed by the 3D nuclei growth. However, a difference between the epitaxial growth of POBA on mica and the commonly observed epitaxial growth of inorganic crystals is that the monolayer POBA oligomer domains have an island-like pattern which leaves the mica surface partially uncovered.

The film thickness of Sample 2 (mica) is about 80–100 nm according to an *FT*i.r. spectra estimation. We reported that the long axis of the long ribbon-like structure was oriented along the [100] and [110] axes mica. A TEM photograph of Sample 2 in *Figure 7* shows that the long crystal domains are oriented in two directions at a 60° angle from each other, which is consistent with the previous result[6]. The size of domains with uniform uniaxial orientation ranges from 800 to 1300 nm in the *c*-axis direction and from 160 to 380 nm in the cross section.

Corresponding AFM images and their schematic representations are shown in *Figure 8*, respectively. *Figure 8* displays the topological features of POBA orientation domains. The thickness of orientation domains, in which POBA chains align uniaxially, ranges from 10 to 60 nm. Each orientation domain consists of several bundles (*Figure 8c*), which are characterized by relatively smooth surfaces. Often one orientation domain lies on the top of another domain with a different orientation (*Figure 8c*). Some of the surfaces are littered by small irregular lumps.

The crystallization is a lateral growth process in the sense that in-plane crystal growth is much faster than the crystal growth in the direction of film thickness. The phenomenon that one orientation domain lies on the top of another one with different orientation is a result of the lateral crystal growth and domain orientation determined by the upstart 2D nuclei. Presumably the competition between the 2D nucleation and crystal growth favours crystal growth. Thus a subsequent crystal lateral domain with orientation determined during the nucleation often grows over several domains. Some bundles are locally singular domains of which each has a singular interface or in other words a flat surface with lowest free energy.

Another AFM picture of the POBA of Sample 2 (mica) at atomic resolution is shown in *Figure 9*. The POBA interchain spacings in *Figure 9* vary from 0.48 to 0.77 nm, which approximately correspond to the lattice spacings, d_{110} and d_{100} of POBA crystals. The junctions between two different POBA molecular orientation domains found in these AFM pictures are marked by arrows.

Because there are various adsorption patterns of oligomers and oligomer domains on mica and initial oligomer layers do not cover the whole mica surface. The POBA crystal growth may form on the oligomer domains and some may form directly on the mica surface. Also, oligomer domains have an island-like structure which leaves mica surface partially exposed. Therefore, the dispersion and discontinuity of the oligomer domains might be attributed to the lack of one dominating POBA crystallographic plane being parallel to the mica surface.

Figure 10 shows an AFM image of Sample 3 (mica) with POBA film thickness of 300–400 nm. Two long domains are distributed at a 120° angle from each other, as is also observed in the AFM of Sample 2. *Figure 11a* shows the height profile of vicinal planes on the boundary of one domain. The domain thickness ranges generally from 30 to 100 nm. *Figure 11b* shows a large

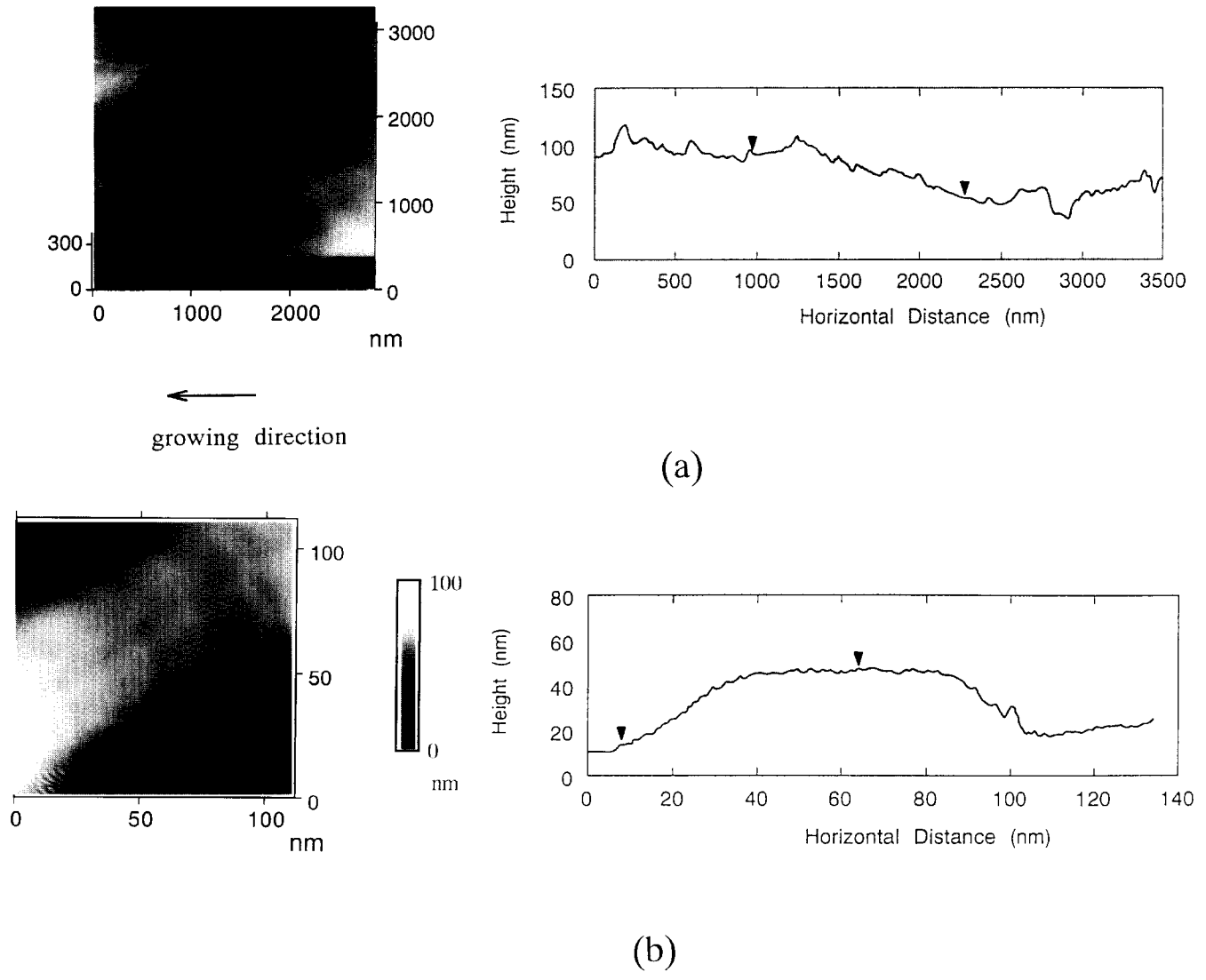

Figure 13 AFM images and height profiles of Sample 5 (KBr). The cross-sectional views between two crosses are shown in the above, where right and left arrows correspond to the crosses

domain with a relatively flat surface with dimension of 1000 nm in contrast to the more bumpy orientation domains in the thin film Sample 2.

The surfaces of the domains in Sample 3 are smoother than the ones in Sample 2, although the scales of the orientation domains in both samples are about the same. The orientation domains in Sample 3 are essentially integrated singular domains albeit the surfaces of singular domains in Sample 3 are rougher than typically perfect singular faces of inorganic single crystals. The roughness in the cross-section tends to be higher than the roughness parallel to the long axis of the domain.

POBA films on KBr substrate

A KBr single crystal has fcc structure with lattice dimension of 0.657 nm. Structurally, K^+ and Br^- ions arrange in alternating positions in the lattice. Cleaving a KBr single crystal often leads to a stepped crystal surface structure.

The epitaxial growth mechanism of POBA on KBr single crystal was found in the previous paper to be such that the three dimensional POBA crystal clusters accumulated directly on the KBr surface, a so-called Volmer–Weber epitaxial nucleation mode.

Figure 12 shows AFM images of Sample 4 (KBr) with a film thickness of 110–150 nm. The AFM images show the long crystal domains with consistent widths of 150–160 nm. The long crystal domains are oriented in four directions forming a 45° angle from each other (*Figure 12a*). This observation is consistent with the results of previous work in which the long axis of the crystal domains was shown to be distributed at a 22.5° angle from the [100] and [010] axes of KBr crystal[6]. The long crystal domains are actually stacked up into multiple layers and consist of many small lateral domains with dimensions of 50–100 nm (*Figures 12b* and *c*). Furthermore, the crystal growth pattern in the unit of small domains tends to extend in the *c*-axis direction before growing in the transverse direction.

Apparently long crystal domains are orientation domains in which the orientation direction of polymer chains is uniform. On the other hand, small domains with smooth surfaces are singular domains which are independent growing units (*Figure 12c*). The dimensions of the orientation domains and the small singular domains are quite consistent and uniform. In addition, the singular domains line up along the long axis of the

crystal domains implying that these singular domains grow in subsequence. Accordingly, the 2D nucleation on the grooves between two singular domains does not occur simultaneous and the nucleation is the controlling step for the crystallization process.

Figure 13 shows the AFM images of Sample 5 (KBr) with a POBA film thickness of 470–640 nm. In *Figure 13a*, the surface is relatively flat over a large area with a scale of 3000 nm instead of the topology of large domains bounded by vicinal planes as observed in the other cases. There are many ridges either parallel or perpendicular to the growing axis.

Figure 13b shows a domain bounded by vicinal planes similar to the one in Sample 3 (mica). However, one vicinal plane of *Figure 13b* is roughened by a seemingly lamina growth and a bump at the location of a laminae is found correspondingly in the profile. There is a possibility that laminae growth occurred on the vicinal plane after the completion of growth of the singular domain.

Growth mechanism

To summarize, most of the homogeneous POBA crystal growth following the initial epitaxial orientations on the single crystalline substrates on mica and KBr feature lateral growth with the *c*-axis parallel to the surface, resulting in layer-like morphology. Because the longest axis of lateral domains in the case of thin film on mica is parallel to the *c*-axis [Sample 2 (mica)] and lateral domains in the case of thin film on KBr tend to extend in the *c*-axis before growing in the transverse direction [Sample 4 (KBr)], the lateral growing rate in the *c*-axis direction is faster than the rate in the transverse direction.

The schemes for the growth process are shown in *Figure 14*. Each orientation domain in the thin POBA films on both mica and KBr substrates consists of many small singular domains, which seem to be independent growing units. The average size of singular domains increases with film thickness. Eventually each orientation domain in the rather thick films consists of one singular domain (*Figures 14a* and *b*).

A plausible explanation for this phenomenon is based on the mechanism of 2D nucleation. Because of the sufficiently dilute monomer concentration and high reaction temperature, a low supersaturation of the oligomers in the system is expected. Also, the morphologies of the POBA lateral crystal domains suggest that the crystal growth processes are largely controlled by the surface diffusion of the growth unit on the crystal-to-solution interface. The total free energy change, ΔF, for the two-dimensional nucleation of POBA can be described in the following equation[10]:

$$\Delta F = -Ad\Delta F_v + A(\gamma_{SL2} - \gamma_{SL1}) + \Delta A\gamma_{SL3} \quad (1)$$

where ΔF_v is the free energy change due to making a unit volume of solid, A and d are the area and height of the nuclei, respectively, γ_{SL1} and γ_{SL2} are the unit free surface energies covered and created by the nuclei, respectively. ΔA is the circumferential area of the nuclei and γ_{SL3} is the unit free surface energy of the nuclei circumference.

According to the above equation, the nuclei that starts a new crystal layer tends to form at high surface energy sites. It is obvious that chain ends are active nucleation sites, which are chemically reactive. Thus the junctions between two unreacted singular domains are the likely sites for the nucleation. Initially, POBA domains epitaxially grown on both mica and KBr are small and discontinuous. As the film thickness increases, some of the vicinal domains sharing the same orientations might be joined by heterogeneous transesterification, which reduces the nucleation sites for the following layer (*Figure 14c*).

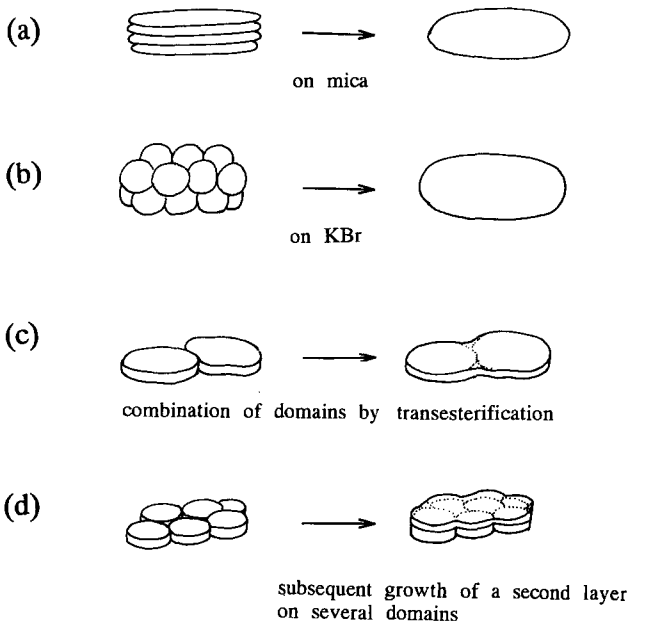

Figure 14 Schematic drawings for the growth mechanism: (a) combination of singular domains on mica; (b) combination of singular domains on KBr; (c) combination of singular domains by transesterification; (d) subsequent overgrowth of POBA layers over several singular domains

Another possibility is due to the competition between the 2D nucleation and the crystal growth. If the crystal growth prevails over 2D nucleation, a subsequent crystal layer often overspreads the several domains (*Figure 14d*). Eventually each orientation domain contains only one singular domain. The preference of the crystal growth in the *c*-axis direction over the transverse direction simply reflects the anisotropic feature of the domain boundary.

CONCLUSIONS

By an AFM investigation, oligomer domains growing epitaxially on mica crystal lattice were found in the vicinity of the nuclei of POBA, which formed the interfacial layer between the mica crystal lattice and homogeneous POBA film. The AFM study of relatively thick films of POBA on mica and KBr substrates revealed the small singular crystal domains composing the big orientation domains in the layered morphology of POBA. The small singular domains with dimensions of 50–100 nm tend to extend in the *c*-axis direction before growing in the transverse direction. Finally, the AFM study of rather thick films of POBA shows that orientation domains become singular domains, some of which are bounded by vicinal planes.

ACKNOWLEDGEMENT

This work was financially supported in part by the

Science and Technology Agency (STA) fellowship program of the Government of Japan.

REFERENCES

1 Bining, G. '10 Years of STM, Proceedings of the Sixth International Conference on Scanning Tunneling Microscopy' (Eds P. Descouts and H. Siegenthaler), North-Holland, Amsterdam, 1992, p. 7
2 Frommer, J. *Angew. Chem. Int. Ed. Engl.* 1992, **31**, 1298
3 Liu, J. and Geil, P. H. *Polymer* 1993, **34**, 1366
4 Lukasheva, N. V., Sariban, A., Mosell, T. and Brickmann, J. *Macromolecules* 1994, **27**, 4726
5 Humel, J. P. and Flory, P. J. *Macromolecules* 1980, **13**, 484
6 Wang, J., Kaito, A., Yase, K. and Tanigaki, N. *Polymer* (in press)
7 Rochow, E. G. 'Comprehensive Inorganic Chemistry', Vol.1, Pergamon Press, Oxford, 1973, p. 1404
8 Nishimura, S., Biggs, S., Scales, P. J., Healy, T. W., Tsunematsu, K. and Tateyama, T. *Langmuir* 1994, **10**, 4554
9 Kern, R., Lelay G. and Metois, J. J. 'Current Topics in Materials Science', (Ed. E. Kaldis), Vol. 3, North-Holland, Amsterdam, 1979, p. 135
10 Brice, J. C. 'The Growth of Crystals From the Melt', Vol.5, North-Holland, Amsterdam, 1965, p. 39